remote sensing

MDPI

Article

Analysis of BDS-3 Onboard Clocks Based on GFZ Precise Clock Products

Tao Geng, Rui Jiang, Yifei Lv * and Xin Xie

GNSS Research Center, Wuhan University, Wuhan 430079, China; gt_gengtao@whu.edu.cn (T.G.); jr_jiangrui@whu.edu.cn (R.J.); xiexin@whu.edu.cn (X.X.)
* Correspondence: lvyifei@whu.edu.cn

Abstract: The characteristics and performance of satellite clocks are important to the positioning, navigation, and timing (PNT) services of Global Navigation Satellite System (GNSS) users. Although China's BeiDou-3 Navigation Satellite System (BDS-3) has been fully operational for more than one year, there is still a lack of comprehensive research on the onboard clocks of the entire BDS-3 constellation. In this study, the precise clock products of GeoForschungsZentrum (GFZ) from day-of-year (DOY) 1, 2021 to DOY 300, 2021 were used to analyze the characteristics and performance of BDS-3 onboard clocks from the following aspects: clock bias, frequency, drift rate, fitting residuals, periodicity, and frequency stability. Compared with BDS-2, the clock quality of BDS-3 satellites has been greatly improved, but there are still jumps in the clock offsets and frequency series of BDS-3 clocks. The drift rate of BDS-3 clocks varies within the range between -2×10^{-18} and 2×10^{-18} s/s^2. The daily model fitting residuals of passive hydrogen masers (PHM) on BDS-3 medium Earth orbit (MEO), inclined geosynchronous orbit (IGSO), and geostationary (GEO) satellites are 0.15, 0.28, and 0.46 ns, respectively. The overlapping Allan deviation (OADEV) of BDS-3 MEO clocks is 4.0×10^{-14} s/s at a time interval of 1000 s. The PHMs on BDS-3 MEO satellites exhibit fewer periodic signals than those of Rb clocks. In addition, the precise clock offsets of the BDS-3 PHMs carried on the MEO, IGSO, and GEO satellites show different periodicities, which are similar to those of the corresponding types of BDS-2 satellites.

Keywords: BeiDou Navigation Satellite System (BDS); satellite clock offset; clock stability; periodic characteristics

Citation: Geng, T.; Jiang, R.; Lv, Y.; Xie, X. Analysis of BDS-3 Onboard Clocks Based on GFZ Precise Clock Products. *Remote Sens.* **2022**, *14*, 1389. https://doi.org/10.3390/rs14061389

Academic Editor: Ali Khenchaf

Received: 20 January 2022
Accepted: 10 March 2022
Published: 13 March 2022

1. Introduction

Satellite time in the GNSS system is established and maintained by satellite onboard clocks, and the performance of satellite clocks directly determines the accuracy of navigation, positioning, and timing services. Therefore, the performance evaluation of satellite onboard clocks is of great significance to GNSS system construction and user service [1].

China's BeiDou-2 Navigation Satellite System (BDS-2) has officially provided services to the Asia–Pacific region since 2012 [2]. Its satellite constellation consists of seven inclined geosynchronous orbit (IGSO), five geostationary (GEO), and three medium Earth orbit (MEO) satellites [3]. All of the BDS-2 satellites are manufactured by the China Academy of Space Technology (CAST). Each satellite is equipped with four high-quality rubidium (Rb) clocks [4]. Performance of BDS-2 onboard clocks has been widely studied. The clock model fitting accuracy is about 0.4 ns [5], which is worse than that of GPS satellites [6]. The clock drift rate is about 1×10^{-13} s/day [7]. Daily frequency stability can reach a level of 10^{-14} [8]. From 2013 to 2018, an atomic clock switch was detected on all BDS-2 satellites, which indicated that BDS satellites needed further improvements in clock quality [5].

To improve the service performance of atomic clocks, new generation high-precision Rb clocks and passive hydrogen masers (PHM) have been equipped on BDS-3 experimental (BDS-3e) satellites and subsequent BDS-3 satellites [9–11]. The BDS-3 constellation

consists of three GEO, twenty-four MEO, and three IGSO satellites, which were developed and manufactured by CAST and the Shanghai Engineering Centre for Microsatellites (SECM) [9,10]. With construction of the BDS-3 system, some initial studies were carried out on the performance of the BDS-3e and BDS-3 MEO satellite onboard clocks [12–17]. The drift rate of Rb clocks on the BDS-3 MEO satellite is about 1.15×10^{-18} s/s and that of the PHMs is 3.15×10^{-19} s/s, which are 7.5% and 73% less than that of BDS-2 Rb clocks, respectively [14]. The noise level of BDS-3 MEO clocks evaluated by the daily fitting residuals is about 0.2 ns [15]. Moreover, the 2-hour, 10-hour, and 7-day prediction precisions of BDS-3 PHMs are about 0.3, 0.4, and 2.2 ns, respectively [16]. The daily stability of BDS-3 MEO satellites is about 2–5 $\times 10^{-15}$ s/s [14]. The stability level of the BDS-3 PHMs is comparable to that of the PHMs of the Galileo as well as to the Rb clocks of the GPS Block IIF; meanwhile, the improved BDS-3 Rb clock is comparable to that of the Galileo Rb clock [17]. With the improved stability of BDS-3 satellite clocks, about 70% level positioning accuracy for BDS-3 is better than 0.65 m at 10 min, which is much better than the positioning accuracy of BDS-2 [18].

Although many pieces of research focus on BDS-3 onboard clocks, these studies concentrated on the performance of the clocks equipped in the BDS-3 experimental satellites and the 18 BDS-3 MEO satellites. By the end of 2021, the complete BDS-3 system was officially in operation for more than one year, but few studies analyzed the performance of the three types of BDS-3 satellites' (including IGSOs, MEOs, and GEOs) onboard clocks.

In this paper, the precision clock offset products with an interval of 30 s from day-of-year (DOY) 1, 2021 to DOY 300, 2021 provided by GeoForschungsZentrum (GFZ) are used to evaluate the onboard clock performance of 29 BDS-3 satellites, including IGSOs, MEOs, and GEOs. Performance of BDS-2 clocks is also evaluated for comparison with BDS-3 clocks. Firstly, the long-term clock bias, frequency, drift, and noise are compared and evaluated based on the clock offset data. Then, the fitting residuals of satellite clocks are computed to reflect the noise level of onboard clocks. Furthermore, frequency stability is analyzed, since frequency stability is an important index for evaluating onboard clock characteristics. Moreover, the periodic terms of different onboard clocks are computed and the possible causes corresponding to periodic variations are discussed. Finally, conclusions are drawn based on the evaluation and analysis.

2. Methods and Data Collection

In this section, the precision clock products used and the detailed information of BDS-2/3 satellites are reviewed. Then, the preprocessing method for outlier detection is introduced. Finally, the satellite clock offset model of evaluating the performance of onboard satellite clocks in this paper is presented.

2.1. Data Collection

Although many multi-GNSS experiment (MGEX) analysis centers provide BDS-2/3 precise clock offset products, such as the European Space Agency (ESA), the Center for Orbit Determination in Europe (CODE), Shanghai Astronomical Observatory (SHAO), GFZ, and Wuhan University (WHU), only WHU, GFZ, and ESA provide BDS-3 precise clock offset products. In this paper, the GFZ's precision clock products with an interval of 30 s were selected to analyze the performance and the characteristics of BDS-2/3 satellite clocks. The time span is from DOY 1 to 300, 2021. The detailed information of satellite clock and orbit types are listed in Table 1.

Table 1. Information about BDS-2/3 satellites and clocks.

PRN	Orbit Type	Satellite Type	Clock Type	Launch Date	PRN	Orbit Type	Satellite Type	Clock Type	Launch Date
C01	GEO	BDS-2	Rb	2019.05	C26	MEO	BDS-3	PHM	2018.08
C02	GEO	BDS-2	Rb	2012.10	C27	MEO	BDS-3	PHM	2018.01
C03	GEO	BDS-2	Rb	2016.06	C28	MEO	BDS-3	PHM	2018.01
C04	GEO	BDS-2	Rb	2010.11	C29	MEO	BDS-3	PHM	2018.03
C05	GEO	BDS-2	Rb	2012.02	C30	MEO	BDS-3	PHM	2018.03
C06	IGSO	BDS-2	Rb	2010.08	C32	MEO	BDS-3	Rb	2018.09
C07	IGSO	BDS-2	Rb	2010.12	C33	MEO	BDS-3	Rb	2018.09
C08	IGSO	BDS-2	Rb	2011.04	C34	MEO	BDS-3	PHM	2018.10
C09	IGSO	BDS-2	Rb	2011.07	C35	MEO	BDS-3	PHM	2018.10
C10	IGSO	BDS-2	Rb	2011.12	C36	MEO	BDS-3	Rb	2018.11
C11	MEO	BDS-2	Rb	2012.04	C37	MEO	BDS-3	Rb	2018.11
C12	MEO	BDS-2	Rb	2012.04	C38	IGSO	BDS-3	PHM	2019.04
C13	IGSO	BDS-2	Rb	2016.03	C39	IGSO	BDS-3	PHM	2018.06
C14	MEO	BDS-2	Rb	2012.09	C40	IGSO	BDS-3	PHM	2019.11
C16	IGSO	BDS-2	Rb	2018.07	C41	MEO	BDS-3	PHM	2019.12
C19	MEO	BDS-3	Rb	2017.11	C42	MEO	BDS-3	PHM	2019.12
C20	MEO	BDS-3	Rb	2017.11	C43	MEO	BDS-3	PHM	2019.11
C21	MEO	BDS-3	Rb	2018.02	C44	MEO	BDS-3	PHM	2019.11
C22	MEO	BDS-3	Rb	2018.02	C45	MEO	BDS-3	Rb	2019.09
C23	MEO	BDS-3	Rb	2018.07	C46	MEO	BDS-3	Rb	2019.09
C24	MEO	BDS-3	Rb	2018.07	C59	GEO	BDS-3	PHM	2018.11
C25	MEO	BDS-3	PHM	2018.08	C60	GEO	BDS-3	PHM	2020.03

2.2. Preprocessing for Clock Offsets

Considering that the precise clock offsets are daily estimated and released, the preprocessing of clock offsets for each satellite is conducted day by day. In this paper, the detection and elimination of outliers are divided into two steps. First, the clock offset data are transformed into frequency data. The frequency data are computed by the following equation:

$$f_i = \frac{L_{i+1} - L_i}{\Delta t} \tag{1}$$

where f_i denotes the frequency data at the epoch i; L_{i+1} and L_i denote the clock offset data at the epoch i and at $i + 1$; and Δt denotes the time between epoch i and $i + 1$. Second, the median absolute deviation (MAD) is applied to detect the outliers. Assuming that the clock frequency series is $\{f_i\}$, $i = 1, 2, \ldots, N$, N is the number of the daily frequency series. A deviation limit in terms of the MAD is described as follows [19]:

$$\text{MAD} = \text{Median}\left\{\frac{|f_i - m|}{0.675}\right\} \; m = \text{Median}\{f_i\} \tag{2}$$

where m is the median value of the clock frequency series. The MAD estimator is approximate to the standard deviation for normally distributed data. If the clock frequency value is outside the range of $[m - n \times \text{MAD}, \; m + n \times \text{MAD}]$, it will be marked as an outlier. The integer n is set as 6 in this paper.

2.3. Satellite Clock Offset Model

The clock offset could be described as the coefficients of a quadratic polynomial in a given reference epoch t_0 [20]:

$$L_i = a_0 + a_1(t_i - t_0) + a_2(t_i - t_0)^2 + \delta_i \tag{3}$$

where L_i is the clock offset of the satellite onboard clock at epoch t_i; a_0 denotes the bias parameter; a_1 denotes the clock frequency, where variations can reflect clock stability; a_2

denotes the drift rate, which is used to describe the frequency characteristic variation of the onboard clocks; and δ_i denotes the random error. Therefore, the physical properties of the clock could be evaluated by the long-term series of clock drift rates and the daily fitting residuals. In this paper, these parameters are obtained by using the least square linear regression method. In addition, the root mean square (RMS) is taken as the statistical index for fitting residuals to evaluate the noise level of the satellite onboard clock. The computation of RMS is shown as follows:

$$\mathrm{RMS} = \sqrt{\frac{1}{N}\sum_{i=1}^{N}\delta_i{}^2} \tag{4}$$

where N is the number of fitting residuals per day.

3. Analysis of Long-Term Clock Bias, Frequency, Drift Rate, and Noise

The parameters of clock bias, frequency, and drift rate are key indexes in describing an onboard clock's physical characteristics [21,22]. The clock bias data analyzed in this paper are clock offsets after preprocessing. The clock frequency is obtained by Equation (1). The quadratic polynomial model listed in Section 2.3 is used to fit the daily data of the clock offset and obtain the drift rates and fitting residuals.

3.1. Analysis of Clock Bias Series

The long period series of the precise clock offset of each BDS-2 and BDS-3 satellite are plotted in Figures 1 and 2, respectively. It is obvious that there are clock offset jumps in both BDS-2 and BDS-3 onboard clocks. Generally speaking, the clock offset jumps are mainly caused by the adjustment of the ground control system, the purpose of which is to control the time synchronization error between stations and satellites within a preset threshold [5]. However, these adjustments destroy the continuity and stability of the clock products, resulting in reduced performance for positioning and timing accuracy.

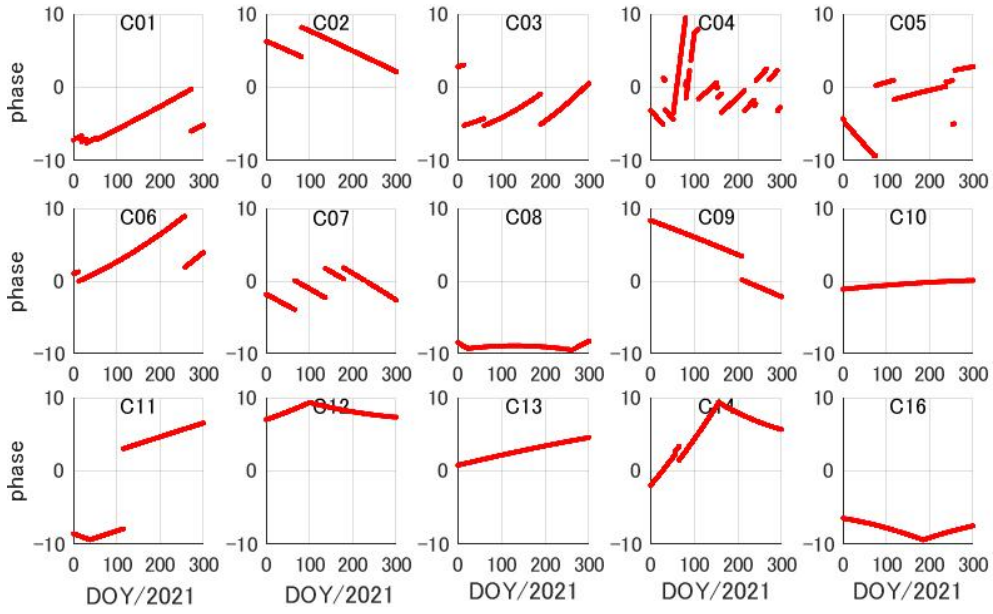

Figure 1. Clock bias series of the BDS-2 onboard clocks from DOY 1 to 300, 2021 (units: 10^{-4} s).

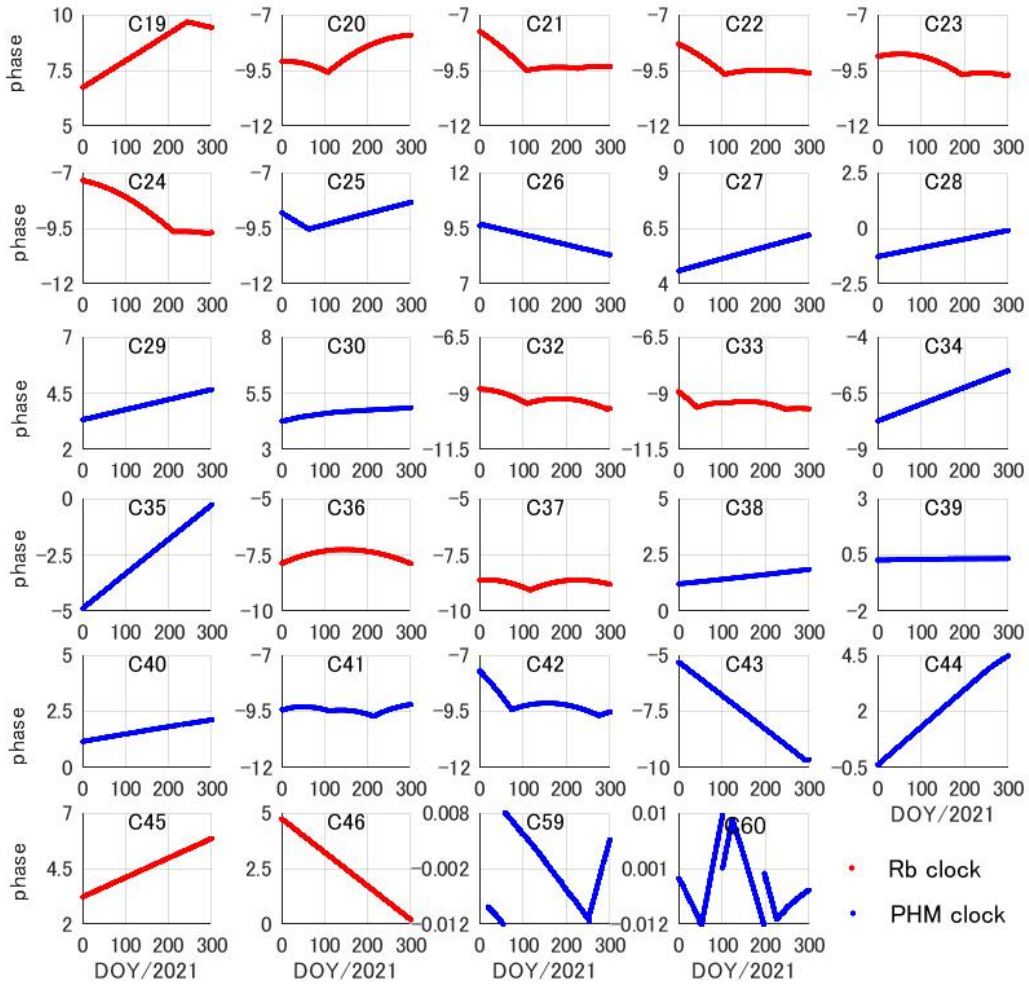

Figure 2. Clock bias series of the BDS-3 onboard clocks from DOY 1 to 300, 2021 (units: 10^{-4} s).

For the BDS-2 onboard clocks shown in Figure 1, the number of jumps of GEO satellite clocks are more than those for IGSO and MEO satellite clocks. In terms of GEO satellites, C01, C03, and C05 are adjusted more than four times, while C04 is adjusted even more than 10 times. In contrast to the GEO satellites, the clock stability of the IGSO and MEO satellites clock bias series are comparable. C06 and C14 are both adjusted fewer than two times. Some satellites, such as C10 and C13, do not even require modulation operations.

In the case of the onboard clocks carried by BDS-3 satellites, it can be seen from Figure 2 that only C59 and C60 (both are PHMs carried on GEO satellites) have jumps, and none of the PHMs and Rb clocks carried on IGSO and MEO satellites experienced jumps. In addition, it can also be seen that the clock bias series of most BDS-3 Rb clocks show a quadratic trend, while those of most of the PHMs show a linear trend. These phenomena indicate that the long-term performance of PHMs is better than Rb clocks.

Comparing Figures 1 and 2, it can be found that the number of jumps of the BDS-2 clocks is far greater than those of the BDS-3 clocks during the research period. This may be a result of clock aging on the BDS-2 satellite, and subsequent cumulative deviations from working in orbit over a longer time.

3.2. Analysis of Frequency Series

Frequency jumps can directly influence the stability of satellite clocks, reducing the accuracy of clock prediction and positioning. The causes of frequency jumps can be mainly attributed to two types of man-made operations. The first operation is when the ground control system adjusts the clock frequency to maintain the accuracy of the satellite clocks.

The second operation is when the clock is switched between the hot backup clock and the working clock.

Figures 3 and 4 compare the long period series of the frequency for BDS-2 and BDS-3 after transferring the clock offset data to frequency data. As depicted in Figures 3 and 4, there are many obvious frequency jumps in the series for both BDS-2 and BDS-3 satellite clocks. For BDS-2 satellites, the frequency of onboard clocks is stable within the range of -10×10^{-11}–10×10^{-11} s/s, except for GEO satellite C04. Most of all onboard BDS-2 satellite clocks experience frequency jumps fewer than two times.

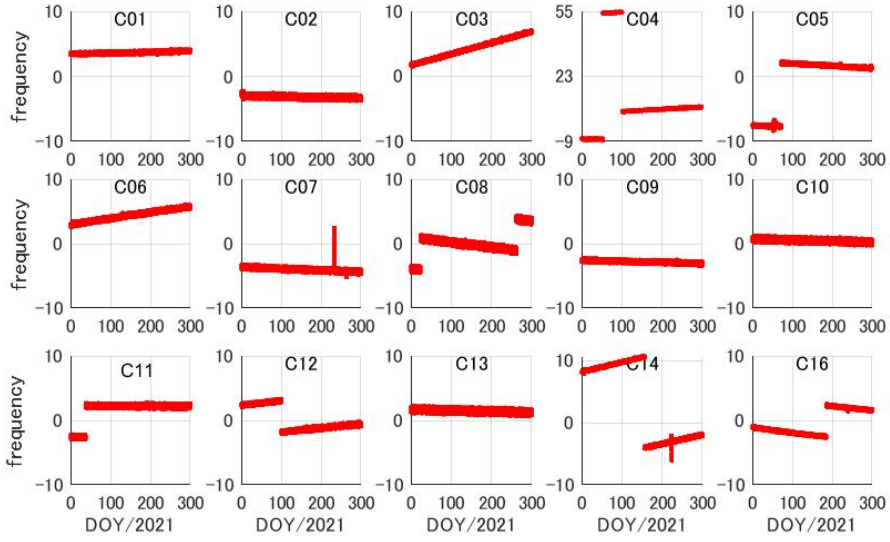

Figure 3. Frequency series of the BDS-2 onboard clocks from DOY 1 to 300, 2021 (units: 10^{-11} s/s).

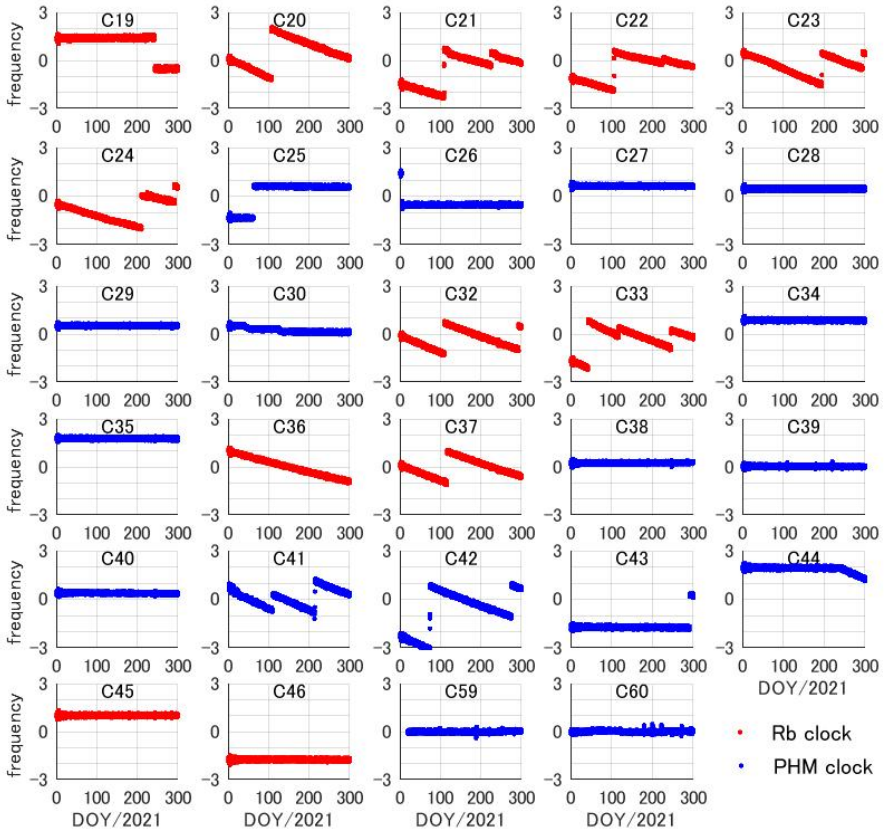

Figure 4. Frequency series of the BDS-3 onboard clocks from DOY 1 to 300, 2021 (units: 10^{-11} s/s).

The frequency series of the BDS-3 satellite onboard clocks provided in Figure 4 show that compared with the BDS-2 system, the frequency series of onboard BDS-3 satellite clocks is between -3×10^{-11} and 3×10^{-11} s/s, which is more continuous and more stable. In the case of the BDS-3 clocks, all Rb clocks have one or two frequency jumps; however, only half of PHMs have any frequency jumps at all. Therefore, PHMs show better continuity of clock frequency than Rb clocks.

3.3. Analysis of Drift Rate Series

The series of clock drift rates for BDS-2 and BDS-3 are shown in Figures 5 and 6. The clock drift rate of BDS-2 onboard clocks is maintained on the order of 10^{-18}, varying from -4×10^{-18} to 4×10^{-18} s/s^2. In addition, it can also be found that the drift rate series of the BDS-2 clock has some fluctuations. The drift rate series of C08, C09, and C10 represent obvious periods, which may be caused by the aging of satellite hardware facilities.

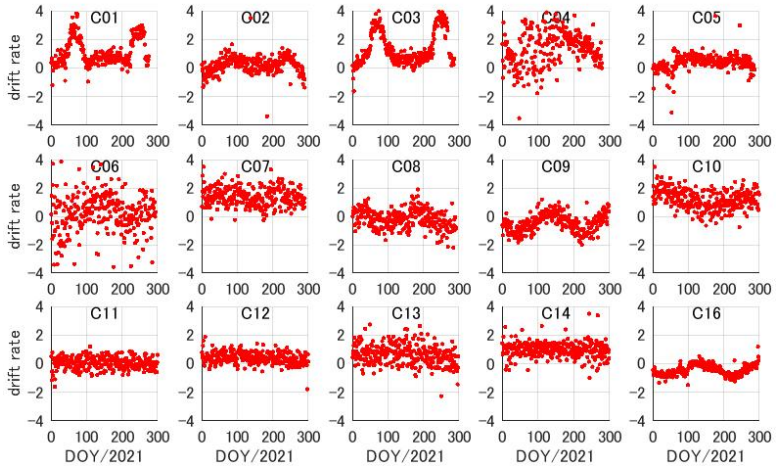

Figure 5. Drift rate series of the BDS-2 onboard clocks from DOY 1 to 300, 2021 (units: 10^{-18} s/s^2).

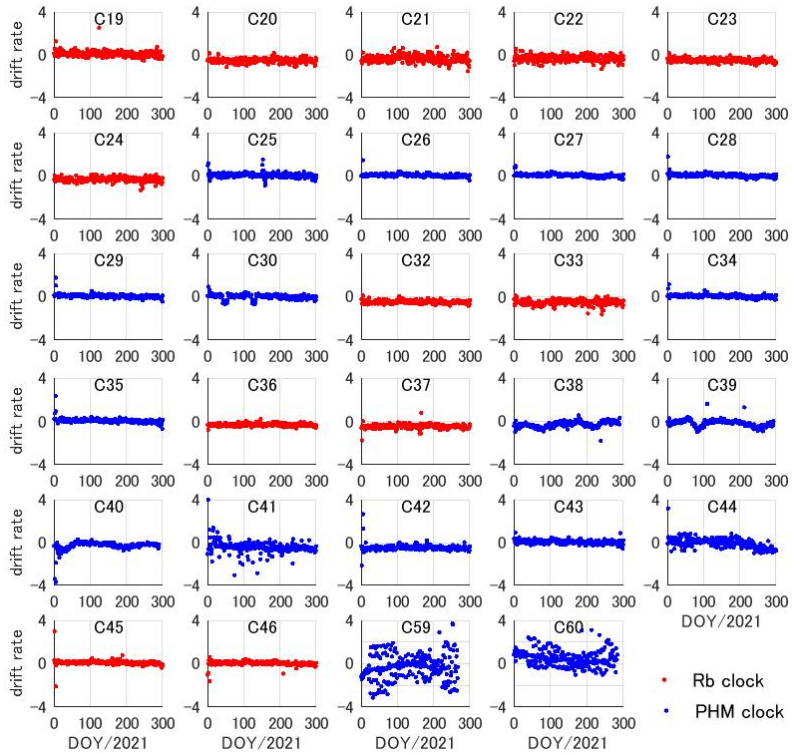

Figure 6. Drift rate series of the BDS-3 onboard clocks from DOY 1 to 300, 2021 (unit: 10^{-18} s/s^2).

Figure 6 plots BDS-3 satellite onboard clock drift rate series. The drift rates of BDS-3 satellite clocks (except two GEO satellites, C59 and C60) vary within the range of -2×10^{-18}–2×10^{-18} s/s^2, which is smaller than that of BDS-2 clocks. Note that the drift rates of C41 and C44 are worse than other PHMs of the MEO satellites, which may have resulted from the lower accuracy of their clock products, since there are only a few MGEX stations that could be employed to track these satellites. Compared to BDS-2 clocks, the drift rate series of BDS-3 onboard clocks show unobvious periodic variations.

3.4. Fitting Precision Analysis of Clock Offset

Figures 7 and 8 show the residual series of BDS-2 and BDS-3 onboard clocks by fitting and removing a daily second-order polynomial. The fitting residuals of BDS-2 are stable within the range of −5–5 ns, while those of BDS-3 are stable within the range of −2–2 ns. The fitting residuals of BDS-3 onboard clocks are overall smaller than those of BDS-2, regardless of clock type. Moreover, it can be seen from Figure 8 that the fitting residuals of clocks on BDS-3 IGSO (C38, C39, C40) and GEO (C59, C60) satellites are greater than those of other BDS-3 satellite onboard clocks subjected to the lower accuracies of orbit estimation of the IGSO and GEO satellites. Note that the residuals of C01, C03, and C04 from DOY 60 to 80, 2021 and from DOY 250 to 300, 2021 are much larger than those of other days.

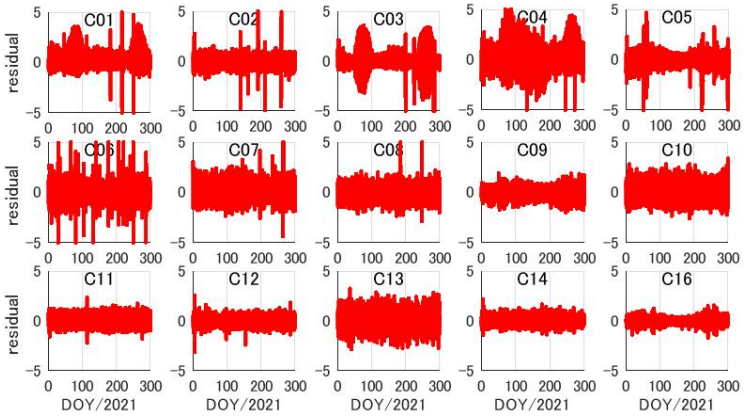

Figure 7. Fitting residual series of the BDS-2 onboard clocks from DOY 1 to 300, 2021 (units: ns).

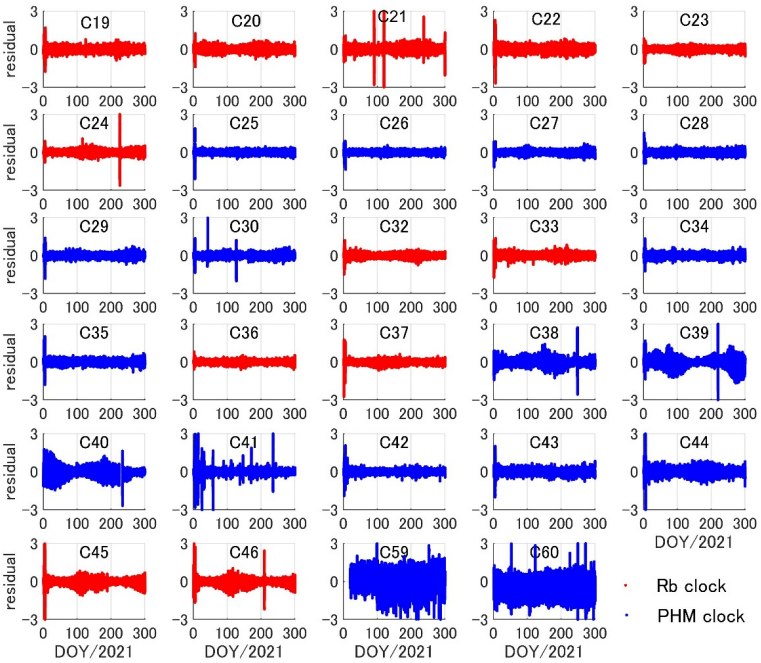

Figure 8. Fitting residual series of the BDS-3 onboard clocks from DOY 1 to 300, 2021 (units: ns).

Figure 9 summarizes the RMS of the daily residuals of BDS-2 and BDS-3 clocks according to the types of orbits and clocks. In terms of BDS-2 onboard clocks, the fitting residual RMS values of the MEO, IGSO, and GEO satellites are 0.33, 0.53, and 0.58 ns, respectively. It is concluded that the daily model fitting residual accuracies of IGSO and GEO are magnitude comparable, while the MEO satellite is better than the other two types. As for the BDS-3 satellite onboard clocks, the RMS value is between 0.15 and 0.46 ns, which is smaller than for the clocks carried on the corresponding types of BDS-2 satellites. It can also be found that the residual of PHMs on BDS-3 MEO satellites is about 0.15 ns, which is slightly better than the residual of BDS-3 Rb clocks. However, the fitting residuals of the PHMs carried by GEO and IGSO satellites increase to 0.46 and 0.28 ns, respectively, which is probably a result of the lower accuracies of their clock products.

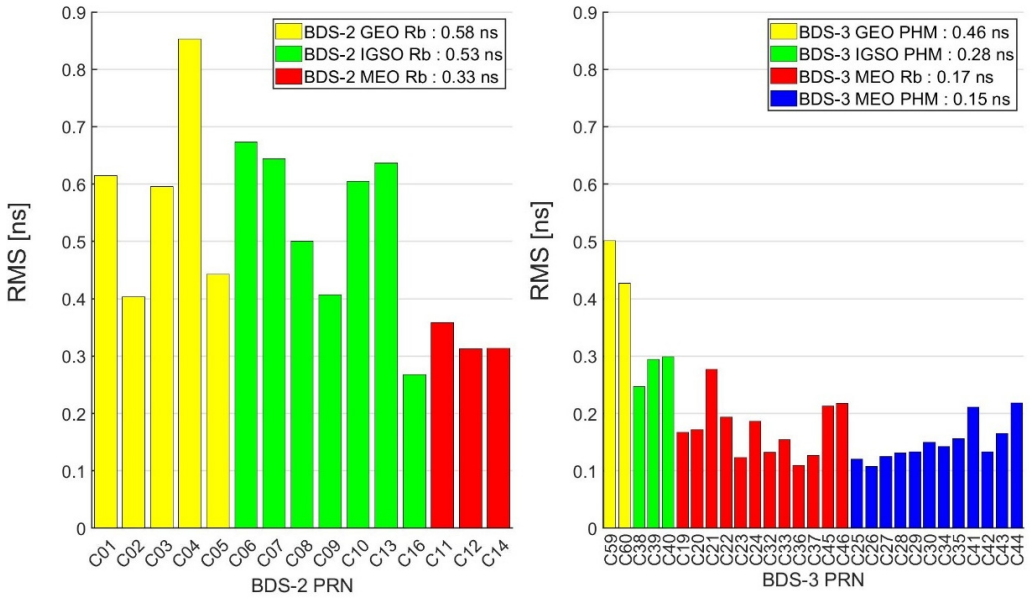

Figure 9. RMS of clock fitting residuals of BDS-2 and BDS-3 GEO, IGSO, and MEO satellites.

4. Frequency Stability Analysis

Clock frequency stability reflects the noise level of the frequency provided by an atomic clock. Allan deviation is a widely used indicator to describe frequency stability and random characteristics. Compared to the classic Allan deviation, the improved overlapping Allan deviation (OADEV) can utilize all possible combinations to calculate variance [23]. The OADEV of a clock at time interval τ can be expressed as:

$$\sigma^2(\tau) = \frac{1}{2(M-2m)\tau^2} \sum_{i=1}^{M-2m} (x_{i+2m} - 2x_{i+m} + x_i)^2 \quad (5)$$

where M is the number of the time series; m is the smoothing factor; and $\tau = m\tau_0$ is the smoothing time. The 300 days of fitting residual data derived from Equation (3) are used to analyze frequency stability.

Figure 10 shows a comparison of the results of frequency stability of different types clocks for BDS-3 over averaging intervals from 30 to 86,400 s. The upper two plots in Figure 10 depict the OADEVs for Rb clocks and PHMs on MEO satellites. Their OADEVs for averaging intervals of 1000 s and shorter decrease with $\tau^{-\frac{1}{2}}$, which corresponds to random-walk phase noise. As the averaging intervals are more than 10,000 s, this trend turns into a power-law variation of τ^{-1}, which corresponds to flicker phase noise [24]. The large broad band of high deviations near 13,600 s and low deviations near 40,000 s may be the response of the OADEV to a 12.88-hour periodic signal. This bump is even more obvious in Rb clocks, which is similar to the bump found in GPS satellites [25,26]. It is also

interesting to note that most Rb clocks and PHMs have very similar performance over the entire range of averaging intervals, except C44, C45, and C46. The spectral analysis of the periodic signal is analyzed in the next section.

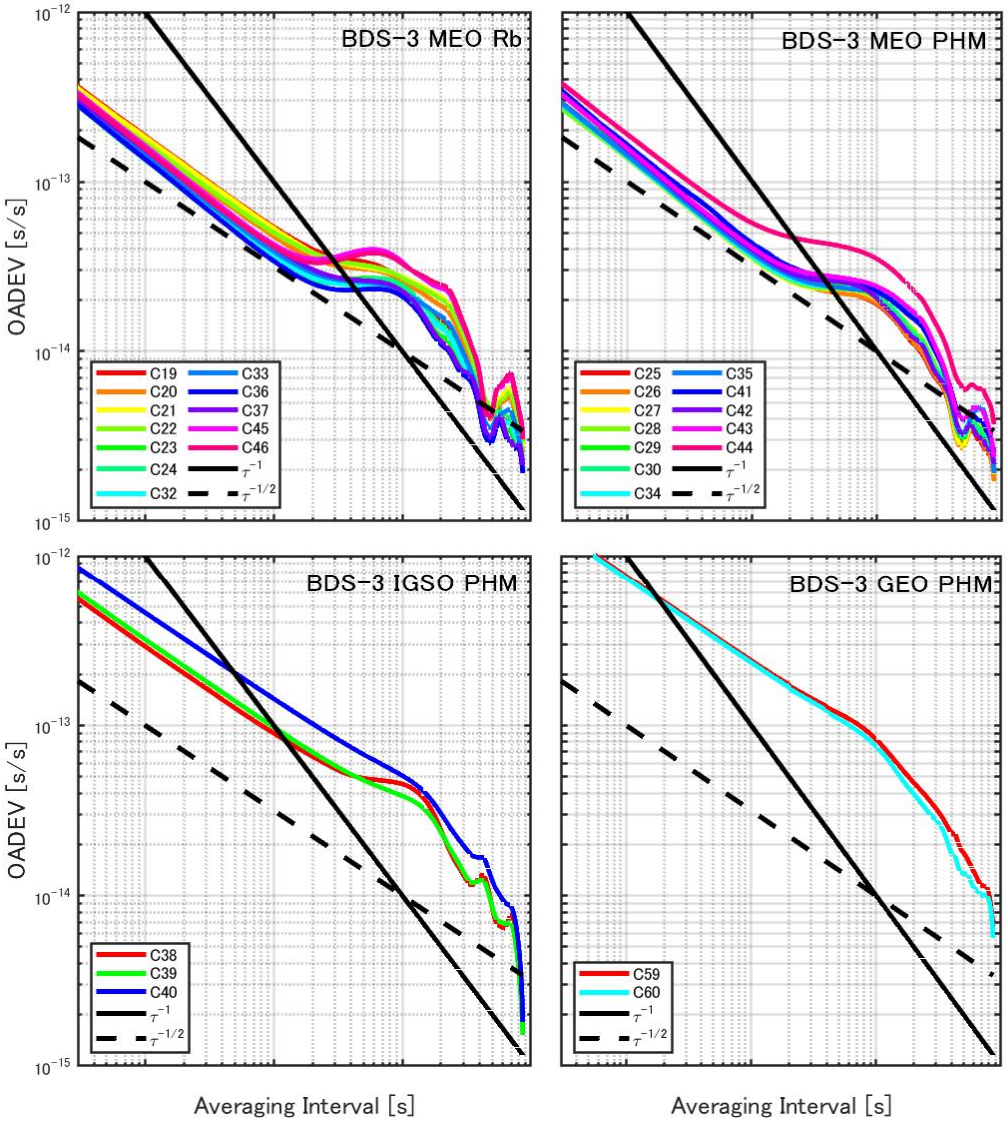

Figure 10. Clock offsets OADEV comparison of different BDS-3 clocks.

The bottom two plots in Figure 10 depict the OADEVs for PHMs on IGSO and GEO satellites. Compared to the PHMs on MEO satellites, the performance is significantly worse over an average interval of 30 to 20,000 s, which is consistent with the corresponding fitting residual data of the three types of satellites. The OADEVs for PHMs on IGSO and GEO follow approximately the same power-law trend within 1000 s as those for PHMs on MEO satellites. Unlike the clocks on MEO satellites, however, there is no large broad band of low or high deviations.

Figure 11 compares the frequency stability of BDS-2 and BDS-3 satellite onboard clocks based on OADEV. It can be seen intuitively that the frequency stability of the BDS-3 satellite clocks is greatly improved over that of BDS-2 satellite clocks. Note that the frequency stability series of C11 fluctuates and oscillates, which differs from the behavior of the rest of the satellites. The same situation has also occurred in others' studies [17]. The reasons for this situation are not clear yet and need to be further studied.

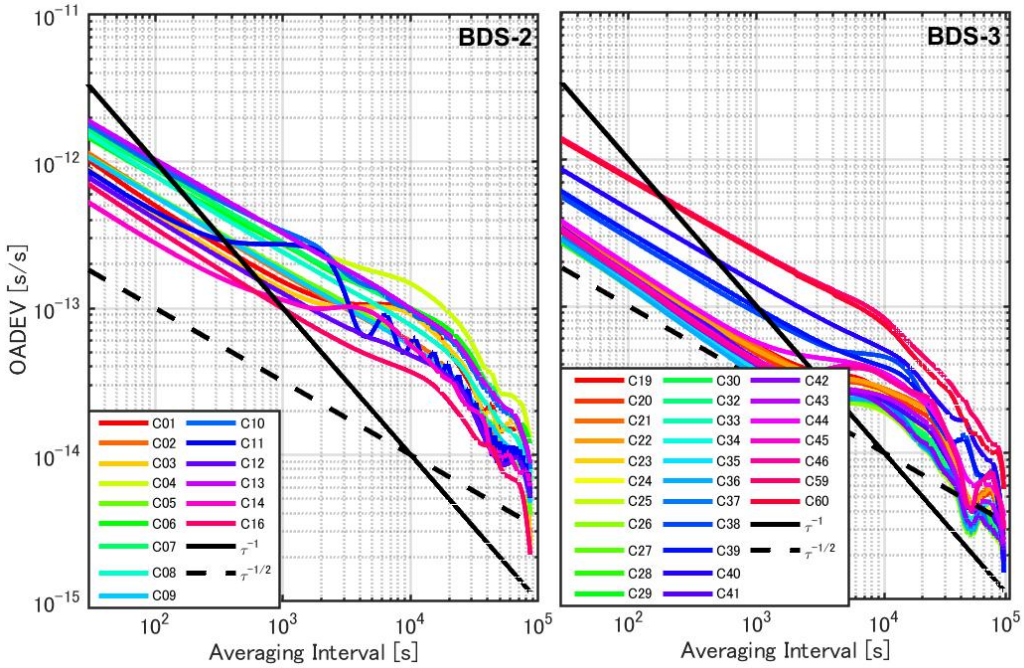

Figure 11. OADEV comparison of BDS-3 and BDS-2 clock offsets.

OADEV at the time intervals of 1000 s, 10,000 s, and 1 day for all BDS clocks are compared in Figure 12. Inspection of the temporal frequency stability for each satellite reveals the following patterns by clock type:

- BDS-3 MEO PHM: These clocks have the best frequency stability at 1000 s and 10,000 s among all BDS clocks. The OADEVs are 4.03×10^{-14}, 2.24×10^{-14}, and 0.22×10^{-14} s/s at 1000 s, 10,000 s, and 1 day, respectively.
- BDS-3 MEO Rb: It can be seen that the stability of MEO Rb clocks is slightly worse than that of BDS-3 MEO PHMs, with the OADEVs being 4.3×10^{-14}, 2.56×10^{-14}, and 0.25×10^{-14} s/s at 1000 s, 10,000 s, and 1 day, respectively.
- BDS-3 IGSO PHM: These clocks have the best daily stability, down to 0.17×10^{-14} s/s, but the stabilities for 1000-second and 10,000-second variations are 11.1×10^{-14} and 4.48×10^{-14} s/s, respectively, which are larger than those of clocks on MEO satellites.
- BDS-3 GEO PHM: Although the newest BDS-3 GEO satellites are equipped with PHMs, their frequency stabilities are much worse than those of MEO clocks, probably resulting from the poor accuracy of precise clock products for GEO satellites. The 1000-second, 10,000-second, and 1-day stabilities are 23.81×10^{-14}, 7.9×10^{-14}, and 0.61×10^{-14} s/s, respectively.
- BDS-2 clocks: Being the older clocks of BDS satellites, their frequency stability is worse than those of BDS-3 clocks. The 1000-second, 10,000-second and 1-day stabilities of BDS-2 satellite onboard clocks are 21.51×10^{-14}, 7.83×10^{-14} and 0.62×10^{-14} s/s, respectively.

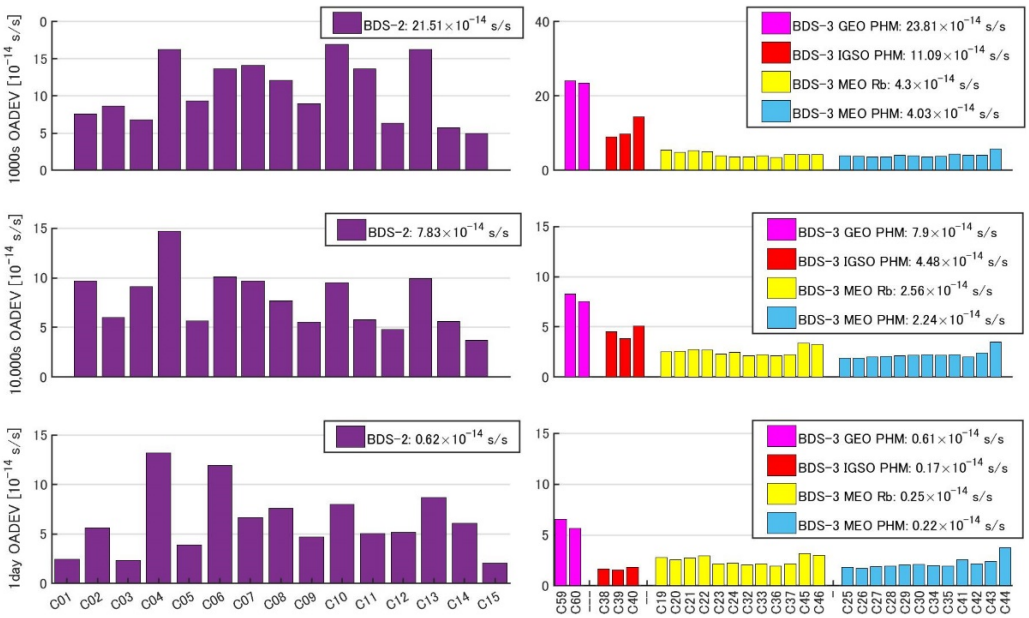

Figure 12. The 1000-second, 10,000-second and 1-day OADEVs of BDS-2 and BDS-3 onboard clocks.

5. Spectrum Analysis

The fast Fourier transform (FFT) method is effective for computing discrete Fourier transforms (DFT). From this, we can judge whether there are periodic changes in time series on the spectrum. The spectral analysis series $X(k)$ at epoch k is described as follows [27]:

$$X(k) = \sum_{n=0}^{N-1} x(n) e^{-j\frac{2\pi}{M}kn} \tag{6}$$

where $x(n)$ is the clock offset fitting residuals fitted by a second-order polynomial; n is the number of an element in the residual series; e is Euler's number; j is an imaginary unit; and M is the number of the time series. However, there are missing samples in the precise clock product, and the elimination of gross errors could influence spectrum analysis. Thus, in this paper, the non-uniform fast Fourier transform (NUFFT) is used to analyze the clock periodical characteristics in the residual series with gaps [28,29]. We use the fitting residuals of Equation (3) to analyze the periodic term, and the corresponding results are shown in Figure 13. The amplitude spectrum is the average value of the same types of satellite clocks, considering that their periodicities are similar.

It can be seen from Figure 13 that the spectral analysis of BDS-2 and BDS-3 clocks show obvious periodicity. The main periods of BDS-2 MEO onboard clocks are about 12.88 (1 cycle per revolution, CPR), 6.44 (2 CPR), and 25.76 h (0.5 CPR), with amplitudes of 0.15, 0.08, and 0.04 ns, respectively. Being different from BDS-2 MEO satellites, the clocks of BDS-2 IGSO and GEO satellites show additional periods that are n times the length of 1 CPR ($n > 2$).

PHMs equipped on BDS-3 IGSO satellites show the same periods as BDS-2 IGSO onboard clocks, but their amplitudes are smaller than those for BDS-2s. The amplitude of 1 CPR is 0.15 ns, which is about two-thirds of the amplitude of that of BDS-2 IGSO onboard clocks. The PHMs equipped on BDS-3 GEO satellites also show the same period as BDS-2 GEO onboard clocks, but their amplitudes are greater than those of BDS-2 clocks. BDS-3 PHMs and Rb clocks aboard MEO satellites have slightly different period characteristics from BDS-2 MEO satellite clocks. The main periods of BDS-3 MEO Rb clocks are 12.88 (1 CPR), 6.44 (2 CPR), and 4.29 h (3 CPR). However, the significant periods of PHMs are about 6.44 (2 CPR) and 12.88 h (1 CPR). There are no n ($n > 2$) CPR periods in both Rb clocks and PHMs. Besides, it can be found that the amplitudes of the period terms of PHMs are significantly smaller than those of Rb clocks.

Since the satellite's clock offset estimated by ground tracking observation may absorb orbit errors, the periodic variation of a BDS-3 onboard clock may be related to the orbital period of the satellite [16,30,31]. According to the results of spectrum analysis, the amplitude of IGSO satellite clocks is much greater than that of the MEO satellite clocks, which is consistent with the poor orbit determination accuracy of the IGSO satellite. In addition, the comparison between BDS-3 PHMs and Rb clocks shows that the performance of PHMs is significantly better than Rb clocks. Furthermore, the performance of BDS-3 satellite clocks is better than that of BDS-2 onboard clocks.

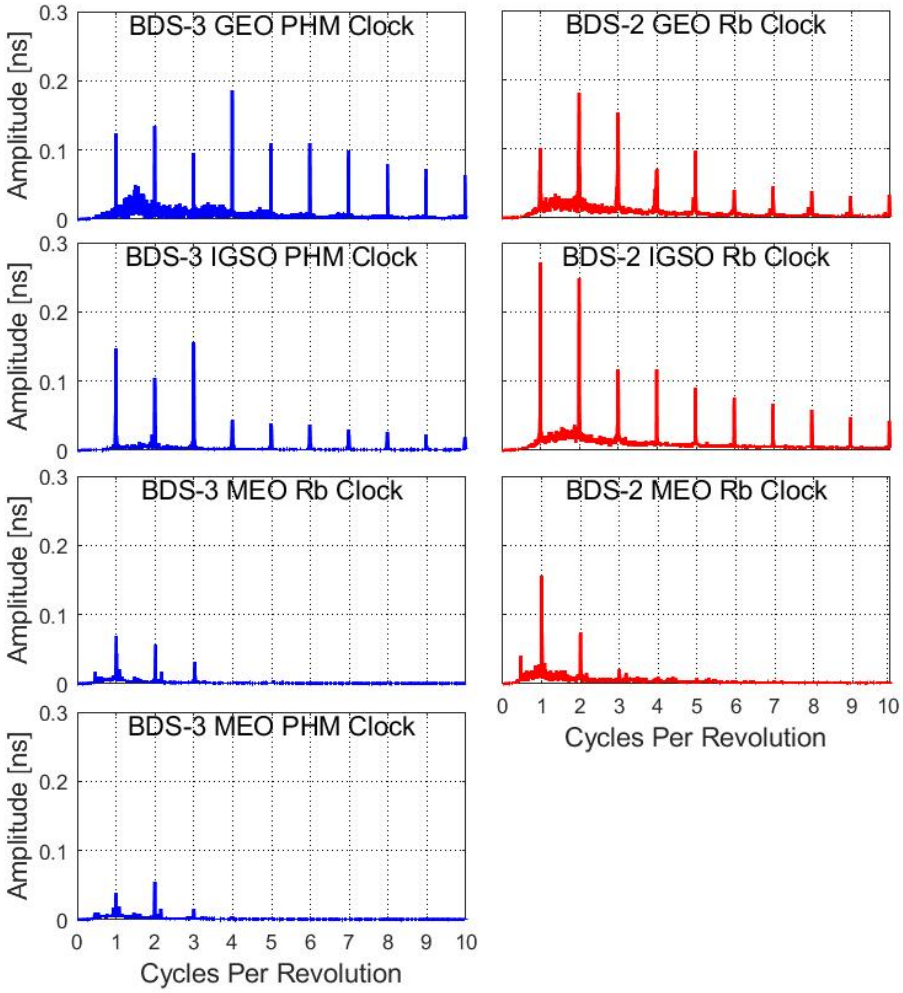

Figure 13. Averaged amplitude spectra of BDS satellite clock offsets.

6. Discussion

According to the above analysis, there are pronounced bumps near 13,600 s in the OADEV plots for both BDS-3 Rb clocks and PHMs. This feature may be the response to the 12.88-h periodic signal lying in the clock series, which is further confirmed in the spectrum analysis. Some researchers have noticed a clear relationship between the orbital dynamics and the periodic signals [16,30]. The orbit errors would be mapped to clock offset estimates when solving for the clock offset in conjunction with orbit parameters due to the correlations between the clock offset and the radial component of the orbit [32]. Therefore, if the influence of orbital errors can be eliminated while solving for the clock offset, the "bump" could be flattened and the OADEV could be reduced. The BDS-3 satellites are equipped with inter-satellite link (ISL) payloads. The realization of BDS-3 ISL technology provides an opportunity for the analysis of the clock with ISL observations [33,34]. The subtraction of bidirectional ISL observations can eliminate the orbit parameters; thus, the estimation of clock offset could mitigate the influences of orbit errors. Compared to the

ground-only clock estimation, the OADEV of the clock estimation using ISL observations is better for averaging intervals longer than 5000 s, and the "bump" is notably flattened [30]. However, ISL observations are access limited and the analysis centers (AC) cannot use them in the production of precise orbits and clocks.

Although orbit error is absorbed in the precise clock, there are some useful conclusions. The results of short-term stability and fitting residuals show that the precise clock of PHMs aboard satellites in different types of orbits has great differences in accuracy. Clock product quality for IGSO and GEO satellites are obviously lower than for MEO satellites. However, this does not prove that clocks equipped on MEO satellites are better than those equipped on IGSO and GEO satellites. As mentioned above, orbit errors may be absorbed into the clock estimates. The GEO satellites have the characteristics of geostationary and higher orbit height, and they can only be tracked by ground stations located in the Asia–Pacific region. The situation of IGSO satellites is also roughly similar. Therefore, the orbit determination accuracy of IGSO and GEO satellites is inferior to that of MEO satellites. The 3D orbit errors of BDS-3 MEO satellites estimated using ground-tracking observation are about 7 cm, which are better than the 3D orbit errors of 15 cm for IGSO satellites and 40 cm for GEO satellites [35]. As a result of that, the estimated clock accuracy of GEO and IGSO satellites is inferior to that of MEO satellites.

The comparison and analysis of long-term clock bias, frequency, drift rate, and noise for BDS-2 and BDS-3 satellites prove that BDS-3 satellites have greatly improved in clock quality. There are two reasons for the improvement of BDS-3 onboard clocks. First, BDS-3 satellites are equipped with more advanced Rb clocks and PHMs. Another reason is that the on-orbit operation time of BDS-2 satellites has been longer than that of BDS-3 satellites, thus the aging of their satellite hardware facilities has been greater.

7. Conclusions

The performance of BDS satellite onboard clocks was analyzed based on the precise clock offset products provided by GFZ from DOY 1, 2021 to DOY 300, 2021. The series of clock bias, frequency, drift rate, and fitting residuals were shown. Moreover, the frequency stability and the periodicity of the clock offsets were analyzed. The following conclusions can be drawn from the results obtained in this paper:

(1) In terms of the BDS-3 system, the performance of PHMs equipped on MEO satellites is slightly better than the performance of Rb clocks. The OADEV of MEO Rb clocks is 4.3×10^{-14} s/s at 1000 s, which is 7% higher than the 4.03×10^{-14} s/s of MEO PHMs. Furthermore, the RMS of fitting residuals of Rb clocks is 0.17 ns, which is 13% higher than that of PHMs.

(2) The precise clock offset products of PHMs carried on BDS satellites show different performances when they operate in different types of orbits. The RMS values of the fitting residuals of PHMs on BDS-3 MEO, IGSO, and GEO satellites are 0.15, 0.28, and 0.46 ns, respectively. Moreover, the 1000-second stabilities of PHMs carried on MEO, IGSO, and GEO satellites are 4.03×10^{-14}, 1.10×10^{-13}, and 2.38×10^{-13} s/s, respectively.

(3) Compared to BDS-2, the BDS-3 satellites show great improvements in clock quality. There are fewer frequency jumps in the long-term performance of BDS-3 onboard clocks. Moreover, the drift rates of BDS-3 satellites clocks varies within the range between -2×10^{-18} and 2×10^{-18} s/s^2, which is less than the range between -4×10^{-18} and 4×10^{-18} s/s^2 for BDS-2 clocks. Furthermore, the RMS of fitting residuals of BDS-2 onboard clocks in GEO, IGSO, and MEO satellites are 0.58, 0.53, and 0.33 ns, respectively, while those of BDS-3 onboard clocks in GEO, IGSO, and MEO satellites are 0.46, 0.28, and 0.16 ns, respectively. The frequency stability of BDS-2 clocks is also worse than that of BDS-3 clocks.

(4) The analysis of the periodicity of BDS onboard clocks shows that there are significant periodic signals in BDS satellite clock offsets. The periodicity of the same types of satellite clocks is similar. BDS-3 with PHMs equipped on IGSO and GEO satellites show the same periodic characteristics as BDS-2 IGSO and GEO Rb clocks. The PHMs

and Rb clocks carried on BDS-3 MEO satellites show different periodic characteristics. The main periods of the BDS-3 MEO Rb clocks are about 12.88 (1 CPR), 6.44 (2 CPR), and 4.29 h (3 CPR). The main periods of the BDS-3 MEO PHMs are about 6.44 (2 CPR) and 12.88 h (1 CPR).

Author Contributions: Conceptualization, T.G.; methodology, T.G., R.J. and Y.L.; validation, R.J. and T.G.; formal analysis, T.G. and R.J.; resources, T.G.; writing—original draft preparation, R.J.; writing—review and editing, Y.L., X.X. and T.G.; supervision, T.G. All authors have read and agreed to the published version of the manuscript.

Funding: This research was financially supported by the National Natural Science Foundation of China (No. 41974036), and the Natural Science Foundation of Hubei Province (No. 2019CFA051).

Institutional Review Board Statement: Not applicable.

Informed Consent Statement: Not applicable.

Data Availability Statement: The clock products are obtained from ftp://igs.ign.fr/pub/igs/products/mgex, accessed on 20 January 2022.

Acknowledgments: International GNSS Service (IGS) and IGS Multi-GNSS Experiment (MGEX) are greatly acknowledged for providing clock products.

Conflicts of Interest: The authors declare no conflict of interest.

References

1. Hessel Barth, A.; Wanninger, L. Short-term Stability of GNSS Satellite Clocks and its Effects on Precise Point Positioning. In Proceedings of the 21st International Technical Meeting of the Satellite Division of The Institute of Navigation (ION GNSS 2008), Savannah, GA, USA, 16–19 September 2008; Volume 3, pp. 1855–1863.
2. CSNO. BeiDou Navigation Satellite System Signal in Space Interface Control Document Open Service Signal B2a (Version 1.0). Available online: http://www.BeiDou.gov.cn/xt/gfxz/201712/P020171226742357364174.pdf (accessed on 17 April 2018).
3. Yang, Y.; Li, J.; Wang, A.; Xu, J.; He, H.; Guo, H.; Shen, J.; Dai, X. Preliminary assessment of the navigation and positioning performance of BeiDou regional navigation satellite system. *Sci. China Earth Sci.* **2013**, *57*, 144–152. [CrossRef]
4. Han, C.; Yang, Y.; Cai, Z. BeiDou Navigation Satellite System and its time scales. *Metrologia* **2011**, *48*, S213–S218. [CrossRef]
5. Huang, G.; Cui, B.; Zhang, Q.; Li, P.; Xie, W. Switching and performance variations of on-orbit BDS satellite clocks. *Adv. Space Res.* **2019**, *63*, 1681–1696. [CrossRef]
6. Huang, G.; Zhang, Q.; Li, H.; Fu, W. Quality variation of GPS satellite clocks on-orbit using IGS clock products. *Adv. Space Res.* **2013**, *51*, 978–987. [CrossRef]
7. Yang, Y.; Tang, J.; Montenbruck, O. Chinese Navigation Satellite Systems. In *Springer Handbook of Global Navigation Satellite Systems*; Teunissen, P.J.G., Montenbruck, O., Eds.; Springer International Publishing: Cham, Switzerland, 2017; pp. 273–304.
8. Wang, B.; Lou, Y.; Liu, J.; Zhao, Q.; Su, X. Analysis of BDS satellite clocks in orbit. *GPS Solut.* **2015**, *20*, 783–794. [CrossRef]
9. Yang, Y.; Mao, Y.; Sun, B. Basic performance and future developments of BeiDou global navigation satellite system. *Satell. Navig.* **2020**, *1*, 1. [CrossRef]
10. Yang, Y.; Gao, W.; Guo, S.; Mao, Y.; Yang, Y. Introduction to BeiDou-3 navigation satellite system. *Navigation* **2019**, *66*, 7–18. [CrossRef]
11. Yang, Y.; Liu, L.; Li, J.; Yang, Y.; Zhang, T.; Mao, Y.; Sun, B.; Ren, X. Featured services and performance of BDS-3. *Sci. Bull.* **2021**, *66*, 2135–2143. [CrossRef]
12. Zhao, Q.; Wang, C.; Guo, J.; Wang, B.; Liu, J. Precise orbit and clock determination for BeiDou-3 experimental satellites with yaw attitude analysis. *GPS Solut.* **2017**, *22*, 4. [CrossRef]
13. Xie, X.; Geng, T.; Zhao, Q.; Liu, J.; Wang, B. Performance of BDS-3: Measurement Quality Analysis, Precise Orbit and Clock Determination. *Sensors* **2017**, *17*, 1233. [CrossRef]
14. Chen, J.; Zhao, X.; Hu, H.; Ya, S.; Zhu, S. Comparison and assessment of long-term performance of BDS-2/BDS-3 satellite atomic clocks. *Meas. Sci. Technol.* **2021**, *32*, 115021. [CrossRef]
15. Wang, W.; Wang, Y.; Yu, C.; Xu, F.; Dou, X. Spaceborne atomic clock performance review of BDS-3 MEO satellites. *Measurement* **2021**, *175*, 109075. [CrossRef]
16. Wu, Z.; Zhou, S.; Hu, X.; Liu, L.; Shuai, T.; Xie, Y.; Tang, C.; Pan, J.; Zhu, L.; Chang, Z. Performance of the BDS3 experimental satellite passive hydrogen maser. *GPS Solut.* **2018**, *22*, 43. [CrossRef]
17. Lv, Y.; Geng, T.; Zhao, Q.; Liu, J. Characteristics of BeiDou-3 Experimental Satellite Clocks. *Remote Sens.* **2018**, *10*, 1847. [CrossRef]
18. Gu, S.; Mao, F.; Gong, X.; Lou, Y.; Xu, X.; Zhou, Y. Evaluation of BDS-2 and BDS-3 Satellite Atomic Clock Products and Their Effects on Positioning. *Remote Sens.* **2021**, *13*, 5041. [CrossRef]

19. Riley, W.; Howe, D.A. *Handbook of Frequency Stability Analysis*; National Institute of Standards and Technology: Gaithersburg, MD, USA, 2008; pp. 89–91.
20. CSNO. BeiDou Navigation Satellite System Signal in Space Interface Control Document Open Service Signal B1C (Version 1.0). Available online: http://www.BeiDou.gov.cn/xt/gfxz/201712/P020171226741342013031.pdf (accessed on 17 April 2018).
21. Huang, G.; Cui, B.; Zhang, Q.; Fu, W.; Li, P. An Improved Predicted Model for BDS Ultra-Rapid Satellite Clock Offsets. *Remote Sens.* **2018**, *10*, 60. [CrossRef]
22. Huang, G.W.; Zhang, Q. Real-time estimation of satellite clock offset using adaptively robust Kalman filter with classified adaptive factors. *GPS Solut.* **2012**, *16*, 531–539. [CrossRef]
23. Huang, G.; Guo, H.; Zhang, J.; Fu, W.; Tian, J. Analysis of the Mid-long Term Characterization for BDS On-orbit Satellite Clocks. *Geomat. Inf. Sci. Wuhan Univ.* **2017**, *42*, 982–988. [CrossRef]
24. Allan, D.W. Time and frequency (time-domain) characterization, estimation, and prediction of precision clocks and oscillators. *IEEE Trans. Ultrason. Ferroelectr. Freq. Control.* **1987**, *34*, 647–654. [CrossRef]
25. Senior, K.L.; Ray, J.R.; Beard, R.L. Characterization of periodic variations in the GPS satellite clocks. *GPS Solut.* **2008**, *12*, 211–225. [CrossRef]
26. Montenbruck, O.; Hugentobler, U.; Dach, R.; Steigenberger, P.; Hauschild, A. Apparent clock variations of the Block IIF-1 (SVN62) GPS satellite. *GPS Solut.* **2011**, *16*, 303–313. [CrossRef]
27. Heckbert, P. Fourier transforms and the fast Fourier transform (FFT) algorithm. *Comput. Graph.* **1995**, *2*, 15–463.
28. Greengard, L.; Lee, J.-Y. Accelerating the Nonuniform Fast Fourier Transform. *SIAM Rev.* **2004**, *46*, 443–454. [CrossRef]
29. Lee, J.-Y.; Greengard, L. The type 3 nonuniform FFT and its applications. *J. Comput. Phys.* **2005**, *206*, 1–5. [CrossRef]
30. Xie, X.; Geng, T.; Zhao, Q.; Lv, Y.; Cai, H.; Liu, J. Orbit and clock analysis of BDS-3 satellites using inter-satellite link observations. *J. Geod.* **2020**, *94*, 64. [CrossRef]
31. Steigenberger, P.; Hugentobler, U.; Loyer, S.; Perosanz, F.; Prange, L.; Dach, R.; Uhlemann, M.; Gendt, G.; Montenbruck, O. Galileo orbit and clock quality of the IGS Multi-GNSS Experiment. *Adv. Space Res.* **2015**, *55*, 269–281. [CrossRef]
32. Hackel, S.; Steigenberger, P.; Hugentobler, U.; Uhlemann, M.; Montenbruck, O. Galileo orbit determination using combined GNSS and SLR observations. *GPS Solut.* **2014**, *19*, 15–25. [CrossRef]
33. Yang, Y.; Yang, Y.; Hu, X.; Chen, J.; Guo, R.; Tang, C.; Zhou, S.; Zhao, L.; Xu, J. Inter-Satellite Link Enhanced Orbit Determination for BeiDou-3. *J. Navig.* **2019**, *73*, 115–130. [CrossRef]
34. Pan, J.; Hu, X.; Zhou, S.; Tang, C.; Wang, D.; Yang, Y.; Dong, W. Full-ISL clock offset estimation and prediction algorithm for BDS3. *GPS Solut.* **2021**, *25*, 140. [CrossRef]
35. Lv, Y.; Geng, T.; Zhao, Q.; Xie, X.; Zhang, F.; Wang, X. Evaluation of BDS-3 Orbit Determination Strategies Using Ground-Tracking and Inter-Satellite Link Observation. *Remote Sens.* **2020**, *12*, 2647. [CrossRef]